JOURNAL OF THE KOREAN ASTRONOMICAL SOCIETY
35: 143 ~ 149, 2002

TEMPORAL CHANGE OF MAGNETIC SHEAR FREE FROM THE 180° AMBIGUITY

Y.-J. MOON[1,2], HAIMIN WANG[1], THOMAS J. SPIROCK[1], AND Y. D. PARK[2]
[1]Big Bear Solar Observatory, NJIT, 40386 North Shore Lane, Big Bear City, CA 92314, USA
E-mail: yjmoon@bbso.njit.edu
[2]Korea Astronomy Observatory, Whaamdong, Yooseong-ku, Daejeon, 305-348, Korea
(Received Aug. 8, 2002; Accepted Aug. 20, 2002)

ABSTRACT

In this paper we present a methodology to derive the temporal change of the magnetic shear angle from a series of vector magnetograms, with a high time cadence. This method looks for the minimum change of the shear angle between a pair of magnetograms, free from the 180° ambiguity, and then accumulates this change over many successive pairs to derive the temporal change of magnetic shear. This methodology will work well if only the successive magnetograms occurred in an active region are well aligned and its helicity sign is reasonably determined. We have applied this methodology to a set of vector magnetograms of NOAA Active Region 9661 on October 19, 2001 by the new digital magnetograph at the Big Bear Solar Observatory (BBSO). For this work we considered well aligned magnetograms whose cross-correlation values are larger than 0.95. As a result, we have confirmed the recent report of Wang et al. that there was the abrupt shear change associated with the X1.6 flare. It is also demonstrated that the shear change map can be an useful tool to highlight the local areas that experienced the abrupt shear change. Finally, we suggest that this observation should be a direct support of the emergence of sheared magnetic fields.

Key words : Sun: magnetic fields—Sun: flare—Sun: photosphere

I. INTRODUCTION

Hagyard et al.(1984) defined the magnetic shear angle as the angular difference between the observed transverse field and the azimuth of the transverse component of the potential field which is computed employing the observed longitudinal field as a boundary condition. That is, the magnetic shear angle θ is given by

$$\theta = \theta_o - \theta_p \,, \tag{1}$$

in which $\theta_o = \arctan(B_{oy}/B_{ox})$ is the azimuth of observed transverse field and $\theta_p = \arctan(B_{px}/B_{py})$ is that of the corresponding potential field component.

Noting that flares are associated with the magnetic shear of strong transverse fields, Wang(1992) proposed a transverse weighted mean shear angle given by

$$\overline{\theta} = \frac{\sum B_t \theta}{\sum B_t} \,, \tag{2}$$

in which B_t is the transverse field strength and the sum is taken over all of the pixels under consideration. He found that the weighted mean shear angle jumped about 5 degrees, coinciding with an X-class flare. He also showed that five additional X-class flares had the same pattern of shear angle variation (Wang et al. 1994 ; Wang 1997). On the other hand, there were apparently contrary reports that the shear may increase, decrease or remain the same after flares (Hagyard et al. 1993 ; Ambastha et al. 1993 ; Hagyard et al. 1999). Chen et al.(1994) showed that there were no detectable changes in magnetic shear after 18 M-class flares. Thus, the temporal change of magnetic shear before and after solar flares still remains controversial.

Most of previous studies on the magnetic shear angle have adopted the potential method for resolving the 180° ambiguity (e.g., Wang et al. 1994). In the potential method, the direction of the transverse field is chosen such that an observed transverse field and the potential field component make an acute angle. However, this criterion may break down for flaring active regions, which generally have strong shears near the polarity inversion line; that is, transverse fields are often nearly parallel to the polarity inversion line.

Let us give one extreme example which results in the wrong estimation of the temporal change of the magnetic shear angle. If the magnetic shear angle, at a position, is changed from 85° to 95°, the potential method gives an estimation of 85° to -85°. This wrong estimation may be corrected by inspecting a sequence of vector magnetograms and comparing them with Hα images. Other elaborate methods for solving the 180° ambiguity (Canfield et al. 1993 ; Metcalf 1994 ; Gary & Demoulin 1995) can be employed. However, these approaches do not guarantee the complete resolution of the ambiguity.

Corresponding Author: Y.-J. Moon

Recently, Big Bear Solar Observatory (BBSO) has upgraded its Digital Vector Magnetograph (DVMG) system, which typically covers an area of about $300'' \times 300''$ with a time cadence of approximately 1 minute. This new system has a much improved sensitivity and resolution compared to that of the old BBSO Videomagnetograph system. The details of the DVMG system have been given by Spirock et al. (2002). Using DVMG vector magnetograms, Wang et al.(2002) reported on two additional X-class flares that showed the shear increase associated with flaring activity.

In this study, we present a method to estimate the temporal change of magnetic shear angle free from the 180° ambiguity. Our method is to minimize the temporal shear change from a series of vector magnetograms with a high time resolution. In addition, we use the shear change map to identify the regions that experienced the abrupt shear changes. In §2, we introduce this methodology. We apply our methodology to a set of BBSO vector magnetograms in §3 and present the results in §4. A brief summary and discussions are delivered in §5.

II. METHODOLOGY

The magnetic shear angle, $\theta(t_i)$ estimated at a time t_i for a given position, can be given by

$$\theta(t_i) = \theta_o(t_i) - \theta_p(t_i), \tag{3}$$

where $\theta_o(t_i)$ includes the 180° ambiguity. Then, the temporal change of the magnetic shear angle between two different times t_i and t_j are

$$\delta\theta_{i,j} = \theta_o(t_j) - \theta_o(t_i) - (\theta_p(t_j) - \theta_p(t_i)). \tag{4}$$

If the observing time difference $(t_j - t_i)$ is much less than the evolutionary time scale of longitudinal field, $\theta_p(t_j)$ is reasonably assumed to be $\theta_p(t_i)$. Since the cadence of the BBSO DVMG magnetograms is about 1 minute, this approximation for the DVMG data is quite satisfactory. It is also noted that the last term should be considered if there are significant changes in flux and field distribution.

Since the change of the shear angle during a short time interval $[t_i, t_j]$ is expected to be small, the temporal change of the shear angle can be minimized like

$$\delta\theta_{i,j} = \mathrm{MIN}_{\mathrm{ABS}}[\theta_o(t_j) - \theta_o(t_i), \theta_o(t_j) - \theta_o(t_i) + 180], \tag{5}$$

where $\mathrm{MIN}_{\mathrm{ABS}}$ is a function which selects a value whose absolute value is the minimum of absolute values and all angles are defined within ±180° to avoid some confusion. This method is effective only if the temporal change of the shear angle is less than 90°. However, this assumption is very solid since a temporal change of magnetic shear angle exceeding 90° has never been reported, and is thought to be impossible in the solar photosphere. It is noted that this quantity has neither been affected by the 180° ambiguity nor any other specific assumptions.

The map of the transverse weighted shear change is given by

$$\delta\overline{\theta}_{i,j}(x,y) = \frac{\overline{B}_t(x,y)\delta\theta_{i,j}(x,y)}{MEAN(\overline{B}_t)}, \tag{6}$$

where $\overline{B}_t$ is the average transverse field of two consecutive magnetograms taken t_i and t_j. To get a reasonable shear change map, the two successive magnetograms should be well aligned each other. In practice, the cross correlation value between the two magnetograms can be used as a criterion for selecting data sets. This map will be used to identify the local areas that experience noticeable shear changes. This quantity can be easily extended to the integral quantity over a whole active region. The change of transverse weighted mean shear angle is given by

$$\delta\overline{\theta}_{i,j} = \frac{\sum \overline{B}_t \delta\theta_{i,j}}{\sum \overline{B}_t}. \tag{7}$$

Since the condition that the change of shear angle is less than 90° is very acceptable in the evolution of solar active regions, this approach may even be applicable to a pair of magnetograms which are taken a few hours (or even longer) apart only if there is no significant difference between the potential fields of the pair of magnetograms.

If a series of magnetograms are continuously observed, we can obtain a continuous change in the transverse weighted shear angle in which each shear change is obtained from a pair of successive magnetograms. Then, the temporal change of the weighted mean shear angle between t_k and t_0 can be described as

$$\overline{\theta}(t_0, t_k) = \sum_{i=0}^{i=k-1} \delta\overline{\theta}_{i,i+1} + (\overline{\theta}_p(t_k) - \overline{\theta}_p(t_0)), \tag{8}$$

whose positive value implies that the shear will increase if the helicity sign of a region of interest is positive, but indicates the shear will decrease if the helicity sign is negative. The last term represents a systematic temporal change of the potential field, which corresponds to the accumulation of the last term in equation (4). The temporal variation of this term should be regarded as a reference. Usually, the helicity sign of an active region can be inferred from the whorl (clock-wise or counter clock-wise) patterns seen in fibril or filament patterns of Hα images and/or in the transverse fields. It is also noted that to determine the helicity sign of the region of interest (mainly near the polarity inversion line) is somewhat different from solving the 180° ambiguity for all considered pixels. Once the helicity sign is determined, equation (8) can be used to detect shear changes free from the 180° ambiguity. Thus we expect that it can be used as an useful tool to examine the temporal change of magnetic shear angle associated with the evolution of active regions.

If the 180° ambiguity of transverse magnetic fields at time t_0 are reasonably solved, the transverse weighted mean shear angle $\overline{\theta}(t_k)$ at a time t_k can be determined like

$$\overline{\theta}(t_k) = \overline{\theta}(t_0) + \overline{\theta}(t_0, t_k) \quad (9)$$

where $\overline{\theta}(t_0)$ is the transverse weighted mean shear angle at t_0. This approach has an advantage which only requires the resolution of 180° ambiguity for the initial magnetogarm taken at t_0, which should be very carefully determined.

III. DATA ANALYSIS

To demonstrate our methodology, we have used a set of BBSO DVMG vector magnetograms of NOAA AR 9661 for which Wang et al.(2002) showed the abrupt shear change associated with the X1.6 flare on October 19, 2001. The DVMG system consists of a 1/4 Å band pass filter, an SMD 1024 × 1024 12-bit CCD camera and three liquid crystals used as polarization analyzers. Each data set consists of four images: 6103 Å filtergram (Stokes-I), line-of-sight magnetogram (Stokes-V) and the transverse magnetograms (Stokes-U and -Q). We usually rebin the camera to 512 × 512 pixels to increase the sensitivity of the magnetograms. After rebinning, the pixel resolution is about 0.6″. The line-of-sight magnetic sensitivity is a few Gauss while the transverse sensitivity is several tens of Gauss. The cadence for a complete set of Stokes images is typically 1 minute. For each vector magnetogram, we correct the cross-talk by scatter plots of Stokes V vs. Q and V vs. U. More detailed descriptions of data analysis are found in Spirock et al.(2002) and Wang et al.(2002).

Wang et al.(2002) resolved the 180-degree ambiguity in the transverse fields by comparing the vector magnetograms with the extrapolated potential fields using the line-of-sight field as the boundary condition. In the present study, we have calculated the temporal change of shear angle for the regions of interest using equation (8) free from the 180° ambiguity. For this work, a series of magnetograms are carefully aligned with each other. To minimize errors due to mis-alignment between a pair of magnetograms, we have only selected pairs of magnetograms whose correlation values are larger than 0.95. For the most cases, the magnetograms are well aligned with high correlation values in the range of 0.97 to 0.99.

Recently, BBSO developed its new generation full-disk Hα system (Denker et al. 1999). This produces 1-minute cadence high resolution images with the 8-inch Singer telescope together with a 2032 × 2032 Apogee Kx4 14-bit digital CCD camera. The pixel size in the images is about 1″, which yields a spatial resolution of 2″. In the present study, BBSO Hα images are used to compare their brightening areas with the regions that experienced the abrupt shear changes.

We have used a pair of 96 minute cadence SOHO/MDI (Scherrer et al. 1995) full-disk longitudinal magnetograms near the flaring time of X1.4 flare to derive the flux change maps. The full disk magnetograms were recorded by a 1024 by 1024 with a pixel size of 2″. The field of view that we analyze is 300″ × 300″, which can cover the whole active regions. The noise levels in the 96-min cadence data are estimated at ~ 14 Gauss per pixel from the comparison of two successive magnetograms. All the magnetograms were aligned by the non-linear mapping, which takes into account the solar differential rotation effect as in Chae(2001) and Chae et al.(2001). It is noted that a time series of magnetograms have their own different geometries to the Sun, which is due to its spherical geometry. Thus this rotational mapping is also effective in such a geometrical foreshortening. Detailed procedures of data analysis are described in Chae(2001) and Moon et al.(2002a). We have determined horizontal velocities by LCT method (November & Simon 1988), which has been commonly used for tracking photospheric intensity patterns such as granulation. For the LCT, there are two important input parameters: FWHM of the apodization window and the time interval between two images for comparison. We select the FWHM of 20″, ten times the spatial pixel size of MDI full disk data. The time interval for horizontal velocity measurement is 96 minutes, which corresponds to about 0.82 pixel when a magnetic flux element moves with a speed of 0.1 km s^{-1}. We assume that the horizontal velocity in the region with low flux density (less than 10 G) or low cross-correlation value (less than 0.9) is zero to reduce the noise effects.

To examine the spatial distribution of flux change, we have devised a method to derive the flux increase and decrease maps from a pair of successive MDI magnetograms. Let us consider a pair of longitudinal magnetograms $B_1(x,y)$ and $B_2(x,y)$ that are taken at two different times, t_1 and t_2, and their difference, $\Delta B(x,y)=B_2(x,y)-B_1(x,y)$. Unless there is significant movement of flux elements, the difference itself can give us the information on flux change. However, it has been noted that there are noticeable photopsheric horizontal motions of magnetic elements, especially associated with flares (Moon et al. 2002a ; 2002b). In deriving the displacements of magnetic elements, the use of SOHO/MDI magnetograms is most appropriate because they are free from the seeing effect and because SOHO has a very stable movement. We make a non-linear mapping to take into account the displacements of moving magnetic features (MMFs) derived from LCT. To reduce the effect of noises and the uncertainty in the non-linear mapping, we make a 3 × 3 binning (6″ × 6″), which is about twice the largest displacement of MMFs. In addition, we only consider flux change whose magnitude is larger than three times the standard deviation of $\Delta B(x,y)$. To avoid an ambiguity in interpretation, flux increase/decrease maps are made not to include the parts in which the longitudinal field has changed its sign. Therefore, the flux increase maps show the parts with $\Delta|B(x,y)| > 0$ and $B_1 B_2 > 0$ while the flux decrease maps show the parts

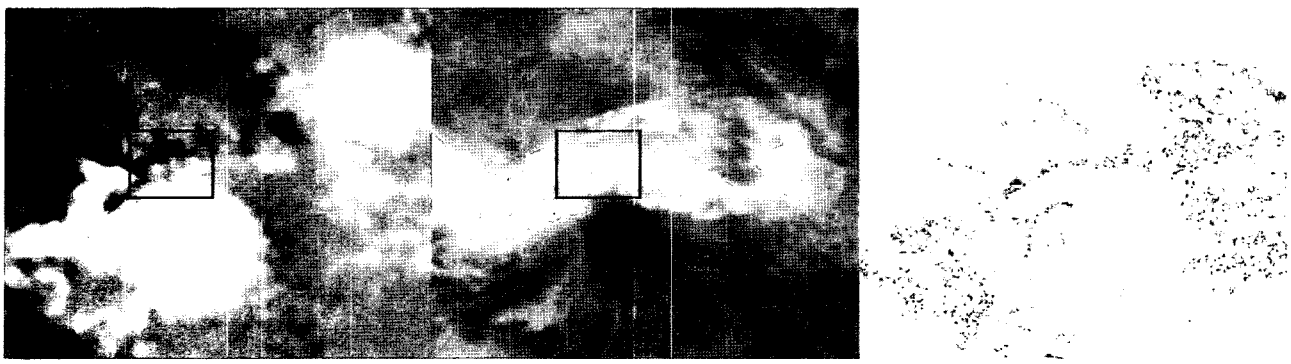

Fig. 1.— Longitudinal magnetogram (left panel), Hα image (middle panel), and a map (right panel) of the shear angle change between 16:20 UT and 16:30 UT for the 2001 October 19 flare event occurred in AR 9661. The field of view is 120″ × 120″. The box marks the area for which the temporal change of transverse weighted shear angle was estimated by Wang et al.(2002). In the shear change map (right panel), bright areas represent the increase of shear and dark areas, the decrease of shear.

with $\Delta|B(x,y)| < 0$ and $B_1 B_2 > 0$. In both maps, white areas (positive values) represent the positive polarity, while black areas (negative values) indicate the negative polarity. We find this method useful in identifying the areas that have undergone the abrupt change of flux.

IV. RESULTS

Figure 1 shows the line-of-sight magnetogram, Hα image, and a map of transverse weighted shear angle change for the 2001 October 19 flare event occurred in NOAA AR 9661. The map of the transverse weighted shear change is made using equation (6) and a pair of magnetograms taken at 16:20 UT and 16:30 UT. As seen in the right panel of Figure 1, the map highlights the local areas that has undergone the abrupt shear change. It is noted that the bright areas experiencing large shear changes are located near the boxed area. We also note that these areas are located near Hα brightenings, which seems to be related to the result of Moon et al.(2002b) who found that the horizontal velocity anomaly associated with the impulsive magnetic helicity injection was found near $H\alpha$ flaring regions.

Our main interest is the boxed area which includes the emerging flux regions in the penumbra of the leading sunspot and the polarity inversion line, which was chosen by Wang et al.(2002) to examine the temporal shear change associated with the X-class flare. The helicity sign for the region is found to be positive, which is inferred from the counter clockwise whorl pattern of vector magnetograms (Fig. 8 of Wang et al. 2002). Figure 2 shows the comparison of Wang et al.(2002) and ours for the temporal change of weighted mean shear angle in the boxed area relative to the initial shear. Our result is qualitatively similar to that of Wang et al.(2002) and further confirms their result that there was an impulsive and permanent shear change near the time of the flare. Our results do not show a monotonic increase of mean shear angle after the flare, which is a little different from Wang et al.(2002). The standard deviation of the shear change during non-flaring times, which is estimated from magnetograms between 16:30 UT and 18:30 UT, is about 1 degree. As seen in dashed line of Figure 2, the temporal variation in the azimuthal component of the potential field, the last term of equation (8), is not significant and its standard deviation is about 0.6 degree. Our methodology should be regarded as a reliable tool since it has removed a few difficulties caused by the 180° ambiguity and the temporal evolution of potential fields.

Figure 3 shows a pair of longitudinal magnetograms taken before and after the flaring time of X-class flare and the flux increase and decrease maps derived from the magnetograms. In the third panel, bright areas highlight the emerging flux regions of positive polarity. As seen in Figures 1 and 3, the local areas that experienced the abrupt shear increase well match the emerging flux regions. This is consistent with the result of Wang et al.(2002) who showed the temporal evolution of magnetic flux in the boxed area. This may be a direct support on the emergence of sheared fluxes. In addition, these results demonstrate that our flux change maps are effective in pinpointing the local areas that have undergone the abrupt change in magnetic flux.

V. SUMMARY AND DISCUSSION

In this paper, we propose a methodology to derive the temporal change of magnetic shear angle without resolving the 180° ambiguity. This method looks for the minimum change of the shear angle between a pair of magnetograms and then accumulates this change over many successive pairs to derive the temporal shear change using a series of vector magnetograms with a high time cadence. We have applied this methodology to a set of high cadence BBSO vector magnetograms of NOAA AR 9661. Major results from the present

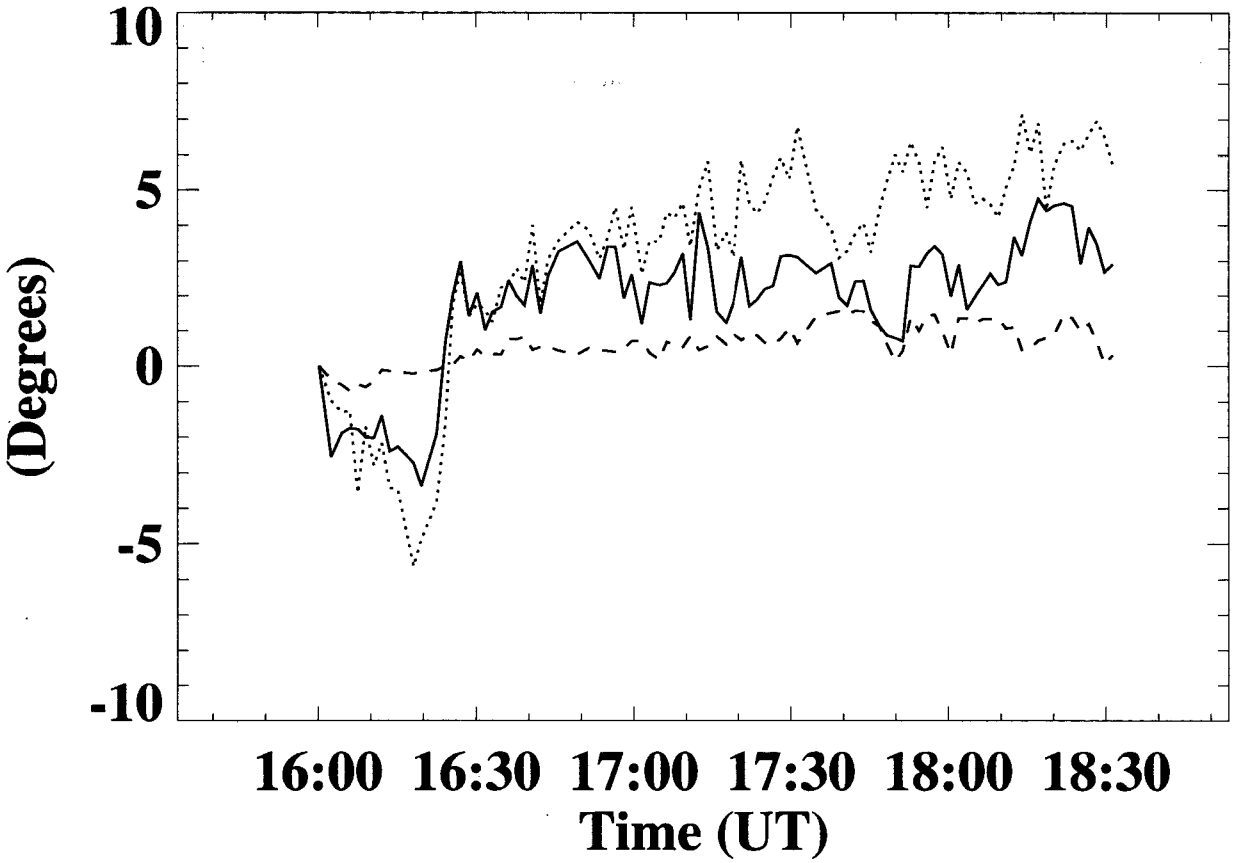

Fig. 2.— Temporal change of the weighted mean shear angle relative to the initial shear angle for the boxed area in Figure 1. The dotted line is what Wang et al.(2002) obtained using the potential method for the 180° ambiguity and the solid line is what we obtained from the present study. The dashed line corresponds to the temporal variation of weighted potential field, the last term of equation (8).

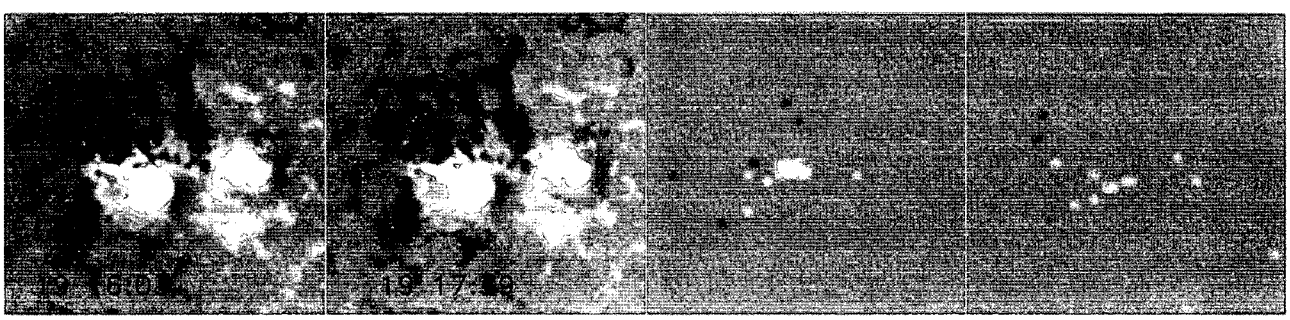

Fig. 3.— Pair of longitudinal magnetograms (left two panels) taken before and after the X1.4 flare and a set of flux increase (third panel) and flux decrease (right panel) maps. The field of view is 300″ × 300″. For both flux change maps, positive values (white) represent the positive polarity, and negative ones (black), the negative polarity.

study can be summarized as follows. (1) Our results are very similar to Wang et al.(2002) and confirm their report that there was an abrupt shear change associated with the X1.6 flare event on October 19, 2001. (2) The shear change map can be used as an useful tool to highlight the local areas that experienced abrupt shear change. (3) The regions that experienced the abrupt shear change correspond to the emerging flux regions, which are also located near the Hα brightenings. This result seems to be a direct support of the emergence of sheared magnetic fields (Wang & Tang 1993). This approach can be extended to other non-potential parameters (for reviews, Moon et al. 2000) such as electric current density, magnetic free energy density, and MAD(Maximum Angular Difference between two adjacent field vectors, Moon et al. 1999).

To deal with the 180° ambiguity, Hagyard et al.(1999) compared the azimuth angle of each magnetogram with the azimuth of a template at every pixel and chose the azimuth closest to that of the template. Their method is conceptually similar to ours. The present method may be a kind of elaboration and extension of their method, but it differs in several aspects. First of all, we have calculated the shear changes between pairs of successive magnetograms and then accumulate them to derive the temporal shear change. Second, we separate the change of azimuth angle from that of the corresponding potential field to distinguish the cause of shear angle change clear. Hagyard et al.(1999) discussed a possibility for errors associated with the potential components derived from longitudinal fields. The above steps are expected to minimize the effect originated from their evolutionary change. Third, we have carefully aligned consecutive magnetograms and used their cross-correlation value as a criterion to select a series of magnetograms. This step is purposed for minimizing several errors such as seeing variation. Fourth, our method can identify shear increase or decrease if the helicity sign for a considered region is reasonably identified.

Recently, we have examined the relationship between magnetic helicity injection rates and solar flares (Moon et al. 2002a ; 2002b). From these studies we found the several cases that showed the impulsive increase of the degree of magnetic helicity during the impulsive variations of helicity change rate associated with major flares. This result seems to be consistent with the present work, together with the previous results on the magnetic shear increase associated with solar major flares (Wang et al. 1994; Wang et al. 2002). It should be noted that such shear increases and impulsive variations of magnetic helicity have been reported only for some strong X-class flares. This tendency is not consistent with a general trend in the evolution of the magnetic fields of active regions (Sakurai & Hiei 1996). We think that there are two explanations for the shear increase: the emergence of sheared fluxes (Wang & Tang 1993) and/or the photospheric response to strong solar flares (Anwar et al. 1993 ; Moon et al. 2002b).

ACKNOWLEDGEMENTS

We are grateful to the BBSO observing staff for their support in obtaining the data. We are very thankful to Dr. J. Chae and Dr. J. Qiu for their valuable comments and discussions. We also thank the referee for his/her valuable comments. This work has been supported by NASA grants NAG5-10894 and NAG5-7837, by MURI grant of AFOSR, by the US-Korea Cooperative Science Program (NSF INT-98-16267), by National Research Laboratory M10104000059-01J000002500 of the Korean government.

REFERENCES

Ambastha, A., Hagyard, M.J., & West, E. A. 1993, Evolutionary and Flare-Associated Magnetic Shear Variations Observed in a Complex Flare-Productive Active Region, Sol. Phys., 148, 277

Anwar, B., Acton, B. W., Hudson, H. S., Makita, M., McClymont, A. N., & Tsuneta, S. 1993, Rapid Sunspot Motion during a Major Flare, Sol. Phys., 147, 287

Canfield, R. C., La Beaujardiere, J.-F., Han, Y., Leka, K. D., McClymont, A. N., Metcalf, T. R., Mickey, D. L., Wuelser, J-P., & Lites, B. W. 1993, The morphology of flare phenomena, magnetic fields, and electric currents in active regions. I - Introduction and methods, ApJ, 411, 362

Chae, J. 2001, Observational Determination of the Rate of Magnetic Helicity Transport through the Solar Surface via the Horizontal Motion of Field Line Footpoints, ApJ, 560, L95

Chae, J., Wang, H., Qiu, J., Goode, P. R., Strous, L., & Yun, H. S. 2001, The Formation of a Prominence in Active Region NOAA 8668. I. SOHO/MDI Observations of Magnetic Field Evolution, ApJ, 560, 476

Chen, J., Wang, H., Zirin, H., & Guoxiang, A. 1994, Observations of vector magnetic fields in flaring active regions, Sol. Phys., 154, 261

Denker, C., Johannesson, A., Marquette, W., Goode, P. R., Wang, H., & Zirin, H. 1999, Synoptic Halpha Full-Disk Observations of the Sun from BigBear Solar Observatory - I. Instrumentation, Image Processing, Data Products, and First Results, Sol. Phys., 184, 87

Gary, G. A. & Demoulin, P. 1995, Reduction, analysis, and properties of electric current systems in solar active regions, ApJ, 445, 982

Hagyard, M. J., Smith, Jr, J. B., Teuber, D., & West, E. A. 1984, A quantitative study relating observed shear in photospheric magnetic fields to repeated flaring, Sol. Phys., 91, 115

Hagyard, M. J., West, E. A., & Smith, J. E. 1993, Magnetic field changes associated with a sub-flare and surge, Sol. Phys., 144,141

Hagyard, M. J., Stark, B. A., & Venkatakrishnan, P. 1999, A Search for Vector Magnetic Field Variations Associated with the M-Class Flares of 10 June 1991 IN AR6659, Sol. Phys., 184, 133

Metcalf, T. R. 1994, Resolving the 180-degree ambiguity in vector magnetic field measurements: The 'minimum' energy solution, Sol. Phys., 155, 235

Moon, Y.-J., Yun, H. S., Lee, S. W., Kim, J.-H., Choe, G. S., Park, Y. D., Ai, G., Zhang, H. Q., Fang, C. 1999, A Measure of Magnetic Field Discontinuity, Sol. Phys., 184, 323

Moon, Y.-J., Yun, H. S., Choe, G. S., Park, Y. D., Mickey, D. L. 2000, Nonpotential Parameters of Solar Active Region AR 5747, JKAS, 33, 47

Moon, Y.-J., Chae, J., Choe, G. S., Wang, H., Park, Y. D., Yun, H. S., Yurchyshyn, V. B., & Good, P. R. 2002a, Flare Activity and Magnetic Helicity Injection by Photospheric Horizontal Motions, ApJ, 574, 1066

Moon, Y.-J., Chae, J., Wang, H., Choe, G. S., & Park, Y. D. 2002b, Impulsive Variations of Magnetic Helicity Change Rate associated with Eruptive Flares, ApJ, in press

November, L. J., & Simon, G. W. 1988, Precise proper-motion measurement of solar granulation, ApJ, 333, 427

Sakurai, T., & Hiei, E. 1996, New observational facts about solar flares from ground-based observations, Adv. Space Res., 17, 91

Scherrer, P. H., Bogart, R. S., Bush, R. I., Hoeksema, J. T., Kosovichev, A. G., Schou, J., Rosenberg, W., Springer, L., Tarbel, T. D., Title, A., Wolfson, C. J., Zayer, I, MDI Engineering Team, 1995, The Solar Oscillation Investigation - Michelson Doppler Imager, Sol. Phys., 162, 129

Spirock, T. J., Yurchyshyn, V. B., & Wang, H. 2002, Rapid Changes in the Longitudinal Magnetic Field Related to the 2001 April 2 X20 Flare, ApJ, 572, 1072

Wang, H. 1992, Evolution of vector magnetic fields and the August 27 1990 X-3 flare, Sol. Phys., 1992, 140, 85

Wang, H. & Tang, F. 1993, Flux emergence and umbra formation after the X-9 flare of 1991 March 22, ApJ, 407, L87

Wang, H., Ewell, M. W., Jr., Zirin, H., & Ai, G. 1994, Vector magnetic field changes associated with X-class flares, ApJ, 424, 436

Wang, H. 1997, Analyses of Vector Magnetograms in Flare-Productive Active Regions, Sol. Phys., 174, 163

Wang, H., Spirock, T. J., Qiu, J., Ji, H., Yurchyshyn, V. B., Moon, Y.-J., Denker, C., & Goode, P. R. 2002, Rapid Changes of Magnetic Fields Associated with Six X-class Flares, ApJ, 576, 497